ACS EARTH AND SPACE CHEMISTRY

http://pubs.acs.org/journal/aesccq

Article

Measurements of Atmospheric Methane Emissions from Stray Gas Migration: A Case Study from the Marcellus Shale

Lauren E. Dennis, Scott J. Richardson, Natasha Miles, Josh Woda, Susan L. Brantley, and Kenneth J. Davis*

Cite This: *ACS Earth Space Chem.* 2022, 6, 909−919

Read Online

ACCESS | Metrics & More | Article Recommendations | Supporting Information

ABSTRACT: Understanding emissions of methane from legacy and ongoing shale gas development requires both regional studies that assess the frequency of emissions and case studies that assess causation. We present the first direct measurements of emissions in a case study of a putatively leaking gas well in the largest shale gas play in the United States. We quantify atmospheric methane emissions in farmland >2 km from the nearest shale gas well cited for casing and cementing issues. We find that emissions are highly heterogeneous as they travel long distances in the subsurface. Emissions were measured near observed patches of dead vegetation and methane bubbling from a stream. An eddy covariance flux tower, chamber flux measurements, and a survey of enhancements of the near-surface methane mole fraction were used to quantify emissions and evaluate the spatial and temporal variability. We combined eddy covariance measurements with the survey of the methane mole fraction to estimate total emissions over the study area (2,800 m^2). Estimated at ∼6 kg CH_4 day^{-1}, emissions were spatially heterogeneous but showed no temporal trends over 6 months. The isotopic signature of the atmospheric CH_4 source ($\delta^{13}CH_4$) was equal to −29‰, consistent with methane of thermogenic origin and similar to the isotopic signature of the gas reported from the nearest shale gas well. While the magnitude of emissions from the potential leak is modest compared to large emitters identified among shale gas production sites, it is large compared to estimates of emissions from single abandoned wells. Since other areas of emissions have been identified close to this putatively leaking well, our estimate of emissions likely represents only a portion of total emissions from this event. More comprehensive quantification will require more extensive spatial and temporal sampling of the locations of gas migration to the surface as well as an investigation into the mechanisms of subsurface gas migration. This work highlights an example of atmospheric methane emissions from potential stray gas migration at a location far from a well pad, and further research should explore the frequency and mechanisms behind these types of events to inform careful and strategic natural gas development.

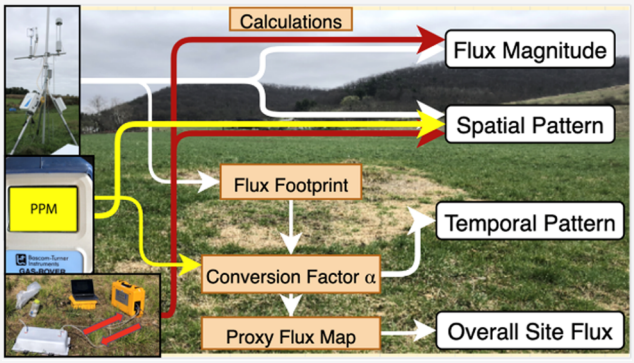

KEYWORDS: *methane leakage, methane emissions, hydraulic fracturing, stray gas, eddy covariance, chamber flux measurements, flux footprint analysis, Marcellus Shale*

INTRODUCTION

Targeting the reduction of methane emissions is an effective component of strategies to mitigate climate change because methane has a radiative forcing 28−36 times that of carbon dioxide over a 100 year period.[1,2] In addition, the global average atmospheric methane mole fraction has increased annually except for three years since 1984 when the U.S. National Oceanic and Atmospheric Administration (U.S. NOAA) began measuring atmospheric methane.[3] Assessment of the anthropogenic contribution to the global methane budget is difficult partly because methane is emitted from multiple sources, both natural and anthropogenic, none of which are well quantified.[1,4] Anthropogenic sources include agriculture, waste management, and fossil fuel production and use.[5] Shale gas development has been of particular interest in the last decades since this new type of fossil fuel production has substantially increased our ability to extract methane from the subsurface.[6] This development utilizes new advances in horizontal drilling and high-pressure, high-volume hydraulic fracturing to extract oil and gas from deep, low-permeability rock such as shale and now represents a significant but poorly quantified source to the atmosphere.[7,8] Anthropogenic releases of previously deeply buried gas derived from high-temperature

Received: September 8, 2021
Revised: March 15, 2022
Accepted: March 17, 2022
Published: April 5, 2022

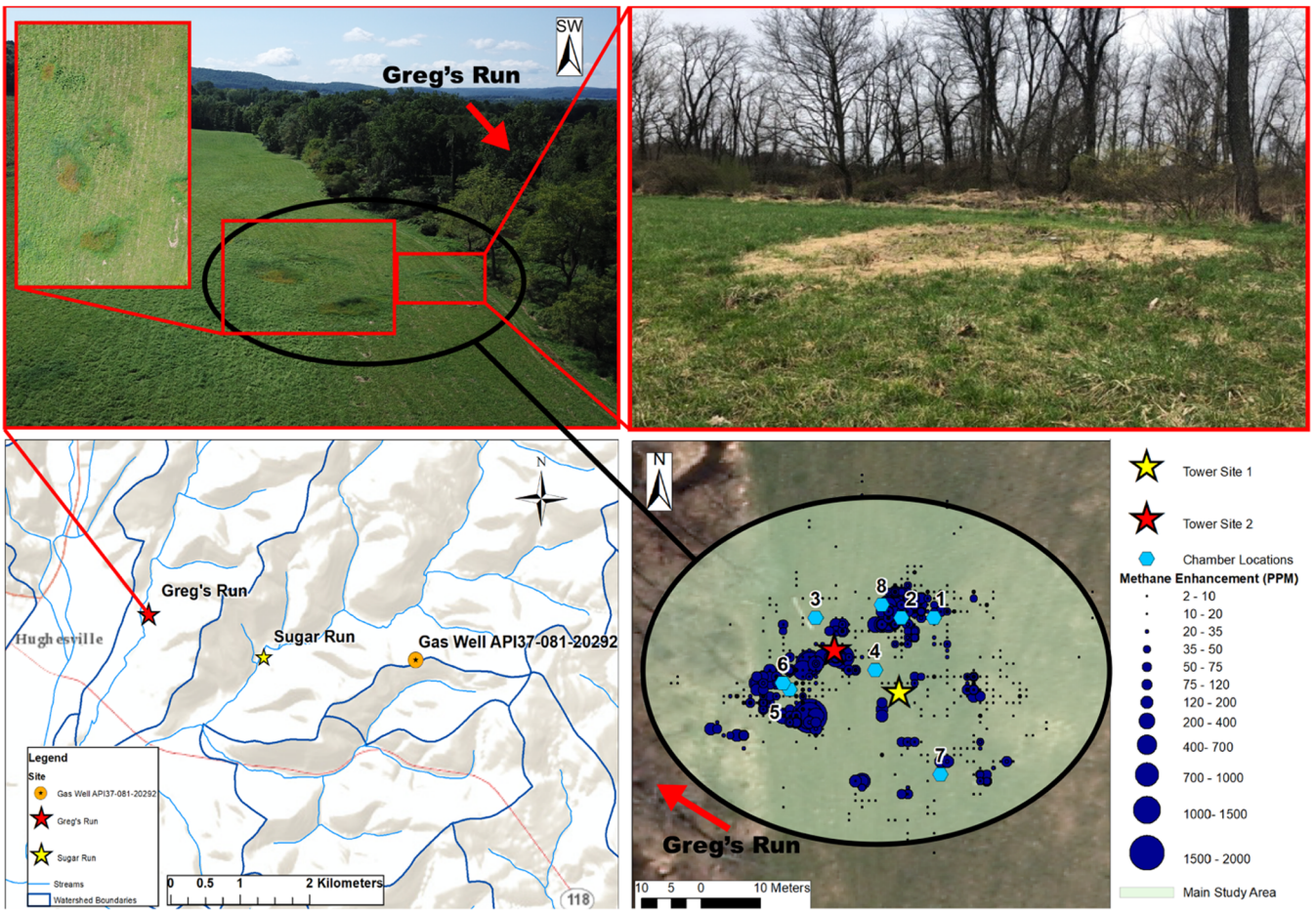

Figure 1. Top left: image looking southwest showing patches of dead vegetation visible at a farm field near Gregs Run. Top right: a closer image of a patch of dead vegetation taken during winter. Bottom left: a map of the sites of interest in this study. Methane bubbles were observed in Gregs Run (near red star) and Sugar Run (yellow star) near Hughesville, PA. A nearby shale gas well (orange circle) has been cited by the Pennsylvania Department of Environmental Protection for integrity issues. Although this well is located greater than 2 km from Gregs Run, it is the closest oil and gas well to this site. As mentioned by Woda et al., 33.3% of unconventional wells within a 13 km × 13 km square centered around Sugar Run have received at least one citation relating to the well integrity.[27] Bottom right: areas of methane emissions as identified by methane mole fraction enhancements measured using a Bascom-Turner Gas-Rover on April 18th, 23rd, and 27th, 2019. Stars indicate the location of the eddy covariance flux tower deployed at site 1 from 12-1-18 to 4-1-19 and site 2 from 4-2-19 to 5-31-19. Hexagons indicate the location of chamber flux measurements, and the study area is denoted by the transparent circle. Gregs Run is located within the trees to the left of the field.

rock processes (so-called thermogenic natural gas) occur in addition to the low natural rates of emission of thermogenic gas in hydrocarbon-rich basins worldwide.[9]

Methane increasingly plays a key role in providing energy for the United States in the form of natural gas, and it has been touted as a bridge fuel to more renewable energy sources.[10] Natural gas production in the United States has increased 4% annually on average from 2006 to 2020, and it is projected to continue to grow through 2050.[11] The Marcellus Shale, found underlying much of Pennsylvania and neighboring states, is one of the main drivers of growth in shale gas production in the United States.[12] While previous extraction targeted reservoirs of migrated gas, horizontal drilling and hydraulic fracturing techniques have allowed gas extraction directly from source rocks that generate methane, such as the Marcellus Shale.[13] Since the first shale gas well was developed in Pennsylvania in 2004, activities associated with natural gas extraction have sometimes released thermogenic methane into the atmosphere.[14] Methane emissions may occur at many points during the extraction and transportation process.[15]

Atmospheric measurements have been used to quantify methane emissions in assessments of gas leakage from operating shale gas well pads. Most of this emission is thought to derive from above-ground gas containment infrastructure, and studies have shown that a high percentage of overall emissions from natural gas extraction come from a small number of high-emitting wells.[16,17] However, given that the state regulator, the Pennsylvania Department of Environmental Protection (PA DEP), cites 1−3% of new shale gas wells for casing or cementing issues as described in the literature,[18] a small fraction of operating shale gas wells could also be leaking at depth and allowing gas migration to the atmosphere. These emissions are not considered in the PA DEP Greenhouse Gas Inventory for the state.[19] The PA DEP Oil and Gas Compliance Report indicates that at least 499 unconventional wells have been cited with a violation related to casing between 2008 and 2021.[20] Although the PA DEP tries to ascertain that casing and cementing problems have been solved, occasionally wells may continue to or may begin to leak long after the violation.[18,21−23] Such wells are not well studied because of the legal difficulties of getting access to sites or data. For example,

https://doi.org/10.1021/acsearthspacechem.1c00312
ACS Earth Space Chem. 2022, 6, 909−919

we are unaware of any documented direct atmospheric measurements of methane emission rates due to subsurface stray gas migration from a problematic shale gas well. Such gas leakage at depth can travel through the water- and air-saturated subsurface and emit into the atmosphere several kilometers from the well pad. Therefore, the prevalence and spatial extent of fugitive gas emission from shale gas wells are largely unknown. Instead, stray gas migration has been simulated,[24] or methane emissions to the atmosphere have been inferred from incidents of methane dissolution into waterways.[25]

Here, we present the first direct atmospheric measurements of emissions of methane at a site of putative stray gas migration. In the scientific literature, this site was first mentioned by Heilweil et al. (2014), in which they study an incident of contamination of water resources by methane in a stream named Sugar Run.[26] The incident occurred near Hughesville in central Pennsylvania after a relatively high density of shale gas wells were emplaced between 2008 and 2012.[27] Woda et al. reported that 33.3% of the 101 spudded wells in the 13 km × 13 km square around latitude 41.23 and longitude −76.60 received one or more violations for casing or cementing issues, which is a higher frequency than statewide estimates.[27] Geological, temporal, geochemical (major element, trace element, long-chain hydrocarbon, isotopic, noble gas), and modeling evidence has been used to establish that the best explanation of contamination of Sugar Run is related to the new shale gas wells nearby.[26−29]

In the small stream of Sugar Run, Heilweil et al. observed bubbles of gas and elevated concentrations of dissolved methane.[25] The PA DEP and researchers investigated this as potential stray gas migration from unconventional natural gas wells located nearby.[21,25,26] Much of the attention has focused on the gas well that is located nearest to Sugar Run, API- 081-20292. Although it is the nearest gas well, it is located over a kilometer from many areas of the stream that have been sampled by researchers. API-081-20292 was drilled between 02/12/11 and 03/17/11 and hydraulically fractured between 06/28/2011 and 07/1/2011.[30] Shut-in pressure tests indicated defective cement in the annuli of the well,[30] and the well was shut in on 6/9/2016 after several issues had ensued (for summary, see Woda et al.).[27] When a well is shut in, it is sealed at the surface and no longer produces. However, if problems at depth remain, it is possible that deep leakage into aquifers continues or even increases. A history of events and casing and cementing violations before 2018 were previously summarized for this well (see Woda et al., 2018 SI); more recent developments are mentioned occasionally on the PA DEP website.[20]

To investigate the incident at Sugar Run, Heilweil et al. used a simple groundwater model to estimate the influx of methane to Sugar Run, and geochemical tracers were used to infer that a thermogenic source of methane is contributing to the elevated concentration.[25,26] Grieve et al. also measured dissolved hydrocarbons and geochemical tracers in Sugar Run and observed many characteristics consistent with the contamination of this stream by nearby leaking wells.[21] In addition, they also estimated the influx of methane into the stream.[21] Woda et al. sampled concentrations of dissolved methane in streams and homeowner water wells at Sugar Run near the shale gas well that was cited by the Pennsylvania Department of Environmental Protection for violations regarding well integrity.[27] They found that the concentrations of ethane and methane in streams and homeowner water wells in this area were elevated compared with predrill concentrations.[27] Ethane is of particular interest in this context because it is rarely if ever found in biogenic natural gas. They hypothesize that the geology of this area, namely, the shallow depth of the Marcellus Shale and the inferred abundance of vertical fractures along the axis of a large fold that dips under the stream, may allow gas to migrate to the surface easily in this area.[27] At a second site of interest along this fold, the Nittany Anticlinorium (Figure 1), a homeowner noticed that patches of dead vegetation began to appear in a farm field on their property in 2015 after the onset of problems in Sugar Run. Images of the progression of dead vegetation can be found in Wen et al.[29] This latter field is more than 2 km away from any shale gas well with casing and cementing violations (Figure 1).[31] The homeowner also noticed intermittent bubbling in a stream named Gregs Run, which parallels the field. The PA DEP discovered up to 100% combustible gas by volume in soil gas samples in the areas of dead vegetation within the farm field.[30] In addition to the problems at Sugar Run, the PA DEP has determined that oil and gas activities impacted the homeowner water well at this property near Gregs Run.[32] Although well API-081-20292 has been cited by the PA DEP for "casing and cementing activities that failed to prevent migration of gas or other fluids into sources of fresh groundwater",[20] no final determination has been made to the best of our knowledge regarding the source of the contamination at the property near Gregs Run.[32]

This study investigates and quantifies atmospheric methane emissions in the aforementioned farm field using eddy covariance flux measurements coupled with chamber flux measurements and a methane mole fraction survey. We quantified both the temporal and spatial variability of the methane fluxes and estimated total emissions from our study site. This work represents the first such attempt to quantify atmospheric methane emissions from a site of putative stray gas migration. In addition to estimating a portion of emissions due to suspected stray gas migration into the farm field, we outline a methodology for combining mole fraction and flux measurements to quantify emissions from similar highly heterogeneous source regions.

METHODS

Site Description. The study site is in Hughesville, Pennsylvania, on privately owned land. The field was previously used to grow crops, but since patches of dead vegetation began to appear around 2014, it was left to lie fallow and is now covered primarily by grass or bare ground. The field itself is flat and surrounded by sloped terrain on the east and by forest to the west. Prevailing winds at a few meters above ground generally come from the north/northeast, likely channeled by the surrounding terrain. Our area of study within the field is approximately 2,800 m^2, which encompasses the average area of the flux footprint of the eddy covariance flux tower (Figure S8).

$\delta^{13}CH_4$ Isotopic Ratio. Measurements of the isotopic ratio of $\delta^{13}CH_4$ can be used in analyses of methane emissions to infer the type of source from which the methane originated.[33] In this study, the isotopic ratio of $\delta^{13}CH_4$ was measured to determine whether methane escaping to the surface at the farm field was of thermogenic or biogenic origin. Thermogenic methane forms when organic matter deep under the Earth's surface is subjected to high pressures and high temperatures, whereas bacteria decompose organic matter at shallow depths

https://doi.org/10.1021/acsearthspacechem.1c00312
ACS Earth Space Chem. 2022, 6, 909−919

to form biogenic methane.[34] Sources that are thermogenic tend to yield gas that has an isotopic ratio that is heavier (less negative) since the methane is enriched in ^{13}C, and sources that are biogenic tend to have an isotopic ratio that is lighter (more negative) because microorganisms preferentially process ^{13}C.[35] For example, Schwietzke et al. found that the global average $\delta^{13}CH_4$ isotopic signatures for fossil fuel sources and biogenic sources are −44.0 and −62.2‰, respectively.[33] The isotopic ratio can vary greatly for fossil fuel sources found at different locations, formations, and at different depths (e.g., Baldassare et al.).[34] For example, in a sample of 234 Marcellus gas wells, the average value of $\delta^{13}C_1$ for Marcellus formation gas found from 0 to 1,000 ft was −43.53‰, whereas gas found from below 5,000 ft had an average isotopic ratio of −32.46‰.[34]

We measured the isotopic ratio using a Cavity Ring Down Spectrometer (G2132-i, Picarro, Inc.), described in Rella et al. and Miles et al.[36,37] The gas inlet was placed about 1 m above ground level, and the gas was transported to the Cavity Ring Down Spectrometer through 30 m polyethylene/aluminum composite tubing (1/4 in. (0.64 cm) OD, Synflex 1300, Eaton Corp.) with a 15 min residence time. The gas samples were not dried, but the water vapor concentration was less than 1.9% during the measurement period, and this causes errors in $\delta^{13}CH_4$ of less than 1‰.[38] The instrument was calibrated in the laboratory using mole fraction-isotopic ratio pairs at 7.3, 6.2, 3.3, and 1.8 ppm and −23.9, −38.3, −54.5, and −66.5‰ $\delta^{13}CH_4$, obtained by mixing zero air with commercially available isotopic standard bottles (Isometric Instruments, Inc.) known to within 0.2‰. The CH_4 mole fraction was corrected for water vapor using methods described in Rella et al.[36] We used a 1 min averaging period, for which the Allan standard deviation is 1‰,[37] and plotted the isotopic ratio on a Keeling plot[37,39] to determine the source isotopic ratio.

We also measured $\delta^{13}CH_4$ (as well as δ D-CH_4) in a water sample collected from a deep domestic water well near Gregs Run on June 4th, 2018. This domestic well was located at the property of the homeowner whose field was sampled in this study. The sample was collected in an Isoflask and analyzed by Isotech, Inc. in accordance with Isotech protocol,[40] following the same protocol as was used for a subset of samples reported by Woda et al.[27]

Emission Pattern Map. A Bascom-Turner Gas-Rover[41] was used to identify areas in which the methane mole fraction was elevated above the background mole fraction both to scope out a location for eddy covariance flux measurements and to create a map of the spatial pattern of emissions to be used in the interpretation of eddy covariance flux measurements. The instrument measures the enhancement of the mole fraction of methane using either catalytic combustion or thermal conductivity (depending on range) with a manufacturer-reported accuracy of ±2% of the sample.[41] The Gas-Rover was calibrated using the automatic calibration system within the instrument with a calibration tank comprised of 2.5% methane before each day of measurements.[41] We surveyed the enhancement of the mole fraction of methane in a grid within a circle of 30 m radius except when forested terrain prohibited measurements (Figure S2). Because the lag time between the Gas-Rover air intake and the mole fraction measurement is ∼5 s, steps of <0.5 m were taken every 5 s. However, the GPS error occasionally caused the point spacing to be slightly less dense (Figure S2). The Gas-Rover inlet was held ∼13 cm above the ground. Survey measurements were linearly interpolated onto a 0.5 m × 0.5 m grid, and the multiple survey data sets were then averaged by grid cell. Surveys of the near-surface mole fraction of methane that were used for analysis were conducted on April 18th, 23rd, and 27th, 2019. The near-surface mole fraction of methane was surveyed with a coarser grid pattern prior to December 2018 to inform the placement of the flux tower.

Eddy Covariance. Methane fluxes were measured using an LI-COR Eddy Covariance system comprised of an LI-7500DS Open Path CO_2 Analyzer, an LI-7700 Open Path CH_4 Analyzer, a Gill WindMaster Pro Sonic Anemometer, and a Vaisala temperature and relative humidity sensor with a radiation shield. Instruments were mounted on a tripod at a height of 3.43 m. The LI-7700 was separated from the sonic anemometer by 76 cm in the southward direction, and the LI-7500DS was separated from the sonic anemometer by 13 cm to the north and 18 cm to the east. Data were collected at a rate of 10 Hz. We calculated fluxes and applied various corrections described below using LI-COR's EddyPro software.[42,43] Additional information about flux processing and corrections is described in the SI. All fluxes measured when the friction velocity was below 0.1 m s^{-1} were discarded to avoid underestimation of the flux due to potential drainage flow in stable conditions (Figure S7). The eddy covariance flux tower was placed at one site from December 1st, 2018 to April 1st, 2019 and later moved to a second site closer to identified areas of emission from April 2nd to May 31st, 2019 (Figure 1).

We calculated flux footprints using a two-dimensional parameterization of the backward Lagrangian stochastic particle dispersion model LPDM-B[44] called the Fast Footprint Parameterization (FFP).[45] This model provides both cross-wind and along-wind components of the flux footprint to determine both the size and shape of the area contributing to the measured flux. FFP assumes that the flow is horizontally homogeneous, but not that the sources/sinks within the footprint are homogeneous.[45] The model also assumes that the flow is statistically stationary over the half-hour averaging period.[45] FFP requires inputs of measurement height, either mean wind speed or roughness length, Obukhov length, friction velocity, the standard deviation of lateral velocity fluctuations, and boundary layer height. Except for the boundary layer height, each input was imported from EddyPro output. Values of the boundary layer height were retrieved from 3 hourly values of the planetary boundary height from the North American Regional Reanalysis (NARR).[46] The simulated boundary layer height was taken from the grid point that most closely matches our measurement site.

Chamber Flux Measurements. To investigate the spatial heterogeneity of the methane fluxes, we constructed and deployed closed, circulating flow flux chambers at eight different locations that fall within the flux tower footprint (Figure 1). The flux chamber design was guided by the USDA-ARS GRACEnet Project Protocols Chapter 3.[47] The chamber system we designed is closed and circulates air between a Los Gatos Ultraportable Greenhouse Gas Analyzer (UGGA) and the chamber, and the buildup of CH_4 over time is measured. With knowledge of the chamber volume and surface area, we calculated a flux (see SI Section 4.2). We calculated the change in CH_4 mole fraction with time using a linear regression. This simplified technique can underestimate the overall flux,[47] but our lack of knowledge of the emission mechanism and process (e.g., diffusion, ebullition, etc.) justifies its use in this instance.[47]

https://doi.org/10.1021/acsearthspacechem.1c00312
ACS Earth Space Chem. 2022, 6, 909−919

The chamber was constructed of a 53 cm × 32.8 cm × 10.2 cm stainless steel steam table pan commonly used for catering. It contains three outlets: a gas intake, a gas outlet, and a small vent to the atmosphere made of nylon compression fittings. The vent allows changes in atmospheric pressure to move gas within the length of a 1/16 inch inner diameter tube while minimizing the loss of methane from the chamber to the atmosphere. A steam table pan with the bottom removed serves as a chamber collar and is inserted into the ground so that a seal with the ground surface and the chamber can be achieved with minimal disturbance to the ground surface during measurement (Figure S12). The chamber collar was inserted approximately 8 cm into the ground at least 24 h before the chamber measurement. Each chamber collar measurement location was chosen based upon the methane mole fraction range measured by the Gas-Rover. Two locations for chamber measurements were chosen based upon a Gas-Rover measurement of methane mole fraction that did not differ from background, and moving forward, we will call these "zero flux" sites (Figure 1, bottom right; chamber sites 3 and 4). We call areas in which the methane mole fraction is elevated and vegetation is visibly dead "hot spots". Two chambers were placed in an identified hot spot southwest of tower site 2 where the methane mole fraction was most elevated (Figure 1, bottom right; chamber sites 5 and 6). Three chambers were placed in a hot spot northeast of tower site 2 (Figure 1, bottom right; chamber sites 1, 2, and 8), and one chamber was placed in a hot spot with occasionally elevated methane mole fraction southeast of tower site 1 (Figure 1, bottom right; chamber site 7). A total of eight chamber measurement locations were measured on five separate days spanning the months of April and May.

The UGGA measures the mole fraction of CH_4, H_2O, and CO_2 using an enhanced cavity absorption technique and has a manufacturer-reported precision of ∼2 ppb over 1 second and ∼0.25 ppb over 100 s for CH_4 within 0.01−100 ppm. For measurements of methane mole fraction higher than this range, the analyzer will measure with a precision of ±1% of the measurement. Prior to measurements, the laser offsets within the UGGA were checked to ensure they were within the absorption lines for CH_4 and H_2O, and before the season of measurements, the UGGA was calibrated using a commercial gas standard. Each chamber measurement was conducted for a period of 5 min. The lag time of gas measurement for the UGGA and associated gas handling system is 10 s. The chamber was attached to the collar 30 s before the measurement period and usually removed 30 s after the 5 min measurement period. On each day of measurements, each chamber flux site was sampled at least twice.

Eddy Covariance, Flux Footprint, and Emission Pattern Map Integration and Interpretation. We estimated the spatial pattern of methane emissions by combining our knowledge of the locations of emissions from the survey of the enhancement of the methane mole fraction with the eddy covariance flux measurements and flux footprints. Prior studies have combined remote-sensing products and flux footprint climatologies to investigate the effects of vegetation heterogeneity on fluxes and flux footprints,[48,49] and in this study, we utilized the measurements of the methane mole fraction to better interpret our fluxes and flux footprints. We hypothesized that the measurements of near-surface enhancement of methane mole fraction are proportional to the methane emission rate. We quantified fluxes based upon this hypothesis with a multiplicative factor, which converts the near-surface methane mole fraction enhancements to a flux. By estimating this multiplier, we can use the methane mole fraction enhancement survey to infer a map of methane emissions.

To do this, we start with eq 1 from Kljun et al.

$$F_c(0, 0, z_m) = \int_D Q_c(x, y) f(x, y) \mathrm{d}x\ \mathrm{d}y \tag{1}$$

where F_c is the measured flux at the tower height and location (μmol m^{-2} s^{-1}), Q_c is a surface source or sink of methane (μmol m^{-2} s^{-1}), f is the footprint function (m^{-2}), x and y are the upwind and cross-wind directions over which the flux footprint is integrated, and D is the area of the Earth's surface over which the integration is performed. Since we do not have direct measurements of Q_c, we instead substitute measurements of the enhancement of the near-surface mole fraction of methane measured with the Gas-Rover and the multiplicative factor (α, μmol ppm^{-1} m^{-2} s^{-1}), which we hypothesize converts the methane mole fraction measured by the Gas-Rover (ppm) to a flux map, Q_c (μmol m^{-2} s^{-1}). We then solve for this multiplicative factor for every eddy covariance flux measurement

$$F_c(0, 0, z_m) = \alpha \int_D M(x, y) f(x, y) \mathrm{d}x\ \mathrm{d}y \tag{2}$$

$$\alpha = \frac{F_c(0, 0, z_m)}{M(x, y) f(x, y) \mathrm{d}x\ \mathrm{d}y} \tag{3}$$

where $M(x, y)$ is the average map of the enhancement of the mole fraction of methane measured by the Gas-Rover. α is calculated for each half-hour flux measurement, and we average α over time for use in the procedure of creating the proxy flux map. In this process, we assume that the emission pattern map created from the Gas-Rover measurements does not change in time. All flux footprints in which the friction velocity is less than <0.1 m s^{-1} are discarded since these low levels of turbulence fall outside of the range tested and validated by Kljun et al.[45]

Proxy Methane Flux Map and Areally Integrated Emission Estimate. We create a proxy flux map by multiplying the Gas-Rover enhancement map, $M(x, y)$, and the temporal average of α. To evaluate the accuracy of this procedure, we compare chamber flux measurements to the appropriate corresponding grid cell of a proxy flux map. Locations of chambers are mapped using the GPS embedded in the Gas-Rover in an attempt to avoid location inconsistencies associated with using multiple positioning systems. We compare calculations of α at two different tower deployment locations to investigate its consistency. We use our estimates of α, which take into account changes over time in the footprint area, to test for changes in methane emissions, Q_c, over time. Finally, we estimate an overall areal methane flux from our study site by integrating over the domain of the proxy flux map. The emissions from each grid cell are summed to get an approximate overall site flux, and we estimate a site level flux with each average α conversion factor that we calculated based on different tower locations and mole fraction enhancement survey maps. To estimate the bounds of uncertainty in this flux, we estimate site emissions using proxy maps calculated from the 10th and 90th percentile values of the distribution of α estimates.

https://doi.org/10.1021/acsearthspacechem.1c00312
ACS Earth Space Chem. 2022, 6, 909−919

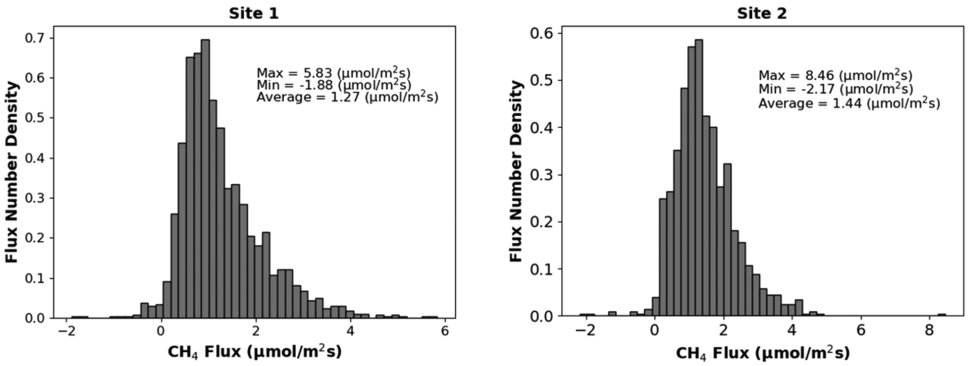

Figure 2. Half-hourly methane flux histograms at site 1 (December 1st, 2018 through April 1st, 2019) and site 2 (April 2nd through May 31st, 2019).

RESULTS AND DISCUSSION

$\delta^{13}CH_4$ Isotopic Ratio. The isotopic ratio of $\delta^{13}CH_4$[37] was measured on May 20th, 2019 in hot spot areas of the field in which we observed methane fluxes to determine whether the methane was of thermogenic or biogenic origin.[35] We determined the source isotopic ratio to be −29‰ (Figure S1). This indicates that the methane is likely thermogenic in origin. Furthermore, this ratio is similar to the source isotopic ratio reported for well API #081-20292 (−28 to −29.5‰, located more than 2 km away from our study site).[27] The methane source isotopic ratio for the homeowner water well near the field was −28.92‰ (δ D −164.2), and nearby homeowner water wells measured by Woda et al. (2018) in 2017 were also similar to our measured ratio (−29.81 and −27.53‰).[27] The PA Department of Environmental Protection has determined that some of these nearby water wells have been impacted by stray gas migration.[32]

Methane Location Survey. The Gas-Rover surveys revealed that methane mole fractions at many locations were much higher than the typical background of around 1.8 ppm;[3] for example, mole fractions approaching 2,000 ppm were measured in some locations (Figure 1). Enhanced methane mole fractions are limited to particular locations, which we call hot spots. Locations of hot spots appeared spatially similar between surveys on a coarse scale (10−20 m^2; Figure S3), which we interpret to mean that the areas of emission are generally constant between survey visits. We used these results to inform the placement of the eddy covariance flux tower and the flux chambers. Some small-scale (~0.5−1 m^2) variations in the location of elevated methane mole fractions between survey measurements were observed on some days (Figure S3). These variations were attributed to GPS error, day-to-day variability in atmospheric turbulence, or small-scale changes in the location of methane emissions. Emissions were often colocated with areas of dead vegetation, but emissions were also measured in other areas.

Flux Magnitude. *Eddy Covariance Fluxes.* The time series of 4,622 half-hour methane fluxes measured with eddy covariance from December 1st, 2018 to May 31st, 2019 (Figure S9) shows persistent emission of CH_4. The average diameter of the flux footprint was ~20 m, which sufficiently sampled most emission hot spots (Figure S8). After conditions with insufficient turbulence with a friction velocity less than 0.1 m s^{-1} were subtracted from this data set (Figure S7), 2,843 half-hour-average eddy covariance fluxes remained. Methane fluxes measured over the 6 month span ranged from −2.17 to 8.46 μmol m^{-2} s^{-1} with an average flux of 1.33 μmol m^{-2} s^{-1}. Fluxes measured at sites 1 and 2 were similar in magnitude and range (Figure 2). We moved the tower to placement site 2 for three reasons: (1) it is located closer to the areas of methane emissions identified with the Gas-Rover, (2) we believed that the prevailing winds would allow the areas of high emission to be sampled more frequently at site 2 (Figure S5), and (3) it provides an assessment of the robustness of the spatial patterns we derive by providing data from a second location. We found that the average flux at site 2 (1.44 μmol m^{-2} s^{-1}) was slightly higher than that at site 1 (1.27 μmol m^{-2} s^{-1}) (Figure 2), probably due to the more frequent sampling of identified hot spots in the second tower location. The distribution of flux measurements is positively skewed (Figure 2), consistent with the heterogeneous distribution of emissions. Other measurements of heterogeneous fluxes, such as measurements of CO_2 emissions related to a volcanic system at Yellowstone,[50] also show a positively skewed distribution.

Chamber Fluxes. Methane fluxes measured with chambers ranged from 0 to 21 μmol m^{-2} s^{-1}, and these fluxes were also spatially heterogeneous (Table 1). The heterogeneity in flux is consistent with the spatial patterns identified by the Gas-Rover surveys of the mole fraction enhancement. Measurements at chamber locations 5 and 6 (see Figure 1 for chamber locations) yielded average fluxes of 7.7 and 3.2 μmol m^{-2} s^{-1}, respectively, while the mean flux at all other sites was less than 1 μmol m^{-2} s^{-1}. Chamber locations 5 and 6 were sampling an area of dead vegetation where we found the greatest enhancement in methane mole fraction in Gas-Rover surveys. The zero flux sites (sites 3 and 4) had methane fluxes

Table 1. Methane Emissions (μmol m^{-2} s^{-1}) from 5 min Chamber Measurements[a]

	mean	standard deviation	maximum	minimum	count
site 1	0.3	0.2	0.5	0	10
site 2	0.9	1.4	3.5	0	8
site 3	0	0	0	0	8
site 4	0	0	0	0	10
site 5	7.7	7.5	21.2	0	10
site 6	3.2	3.8	12.1	0.2	10
site 7	0.7	1	3	0	10
site 8	0.1	0	0.2	0.1	8

[a]Measurements were made at eight locations as shown in Figure 1 on five separate days, with two measurements made on each day. Measurements where leakage was suspected were discarded, as discussed in the Supporting Information.

https://doi.org/10.1021/acsearthspacechem.1c00312
ACS Earth Space Chem. 2022, 6, 909−919

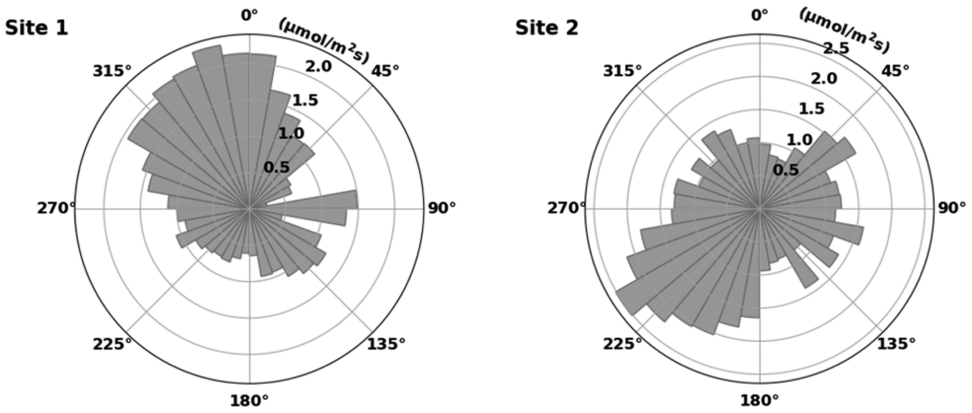

Figure 3. Mean methane fluxes by wind direction at site 1 (left side) from December 1st through April 1st and at site 2 (right side) from April 2nd through May 31st. The polar coordinate is the wind direction in degrees, and the radial coordinate shows the mean methane flux (μmol m^{-2} s^{-1}) in the corresponding binned wind direction.

below the detection limit of our instrument, supporting our hypothesis that background emissions from the field were generally low and elevated fluxes were concentrated in hot spots. Intermediate-magnitude emission sites (1, 2, 7, 8) were those documented as intermediate in magnitude by the near-surface mole fraction data. We see no evidence of small, diffuse methane fluxes throughout the field. All locations, even the hot spots, occasionally emit no measurable methane, suggesting that there is temporal variability in emissions at the resolution of these chambers (~0.2 m^2, 5 min).

Spatial Pattern of Fluxes. *Eddy Covariance Fluxes.* Winds were predominantly out of the northeast and southwest when the tower was deployed at site 1 (December 1st, 2018 to April 1st, 2019) and shifted slightly so that they were more northerly and southerly when the tower was deployed at site 2 (April 2nd to May 31st, 2019) (Figure S5). The largest average methane fluxes measured by eddy covariance at site 1 came from the north/northwest and southeast directions (Figure 3). When comparing these measurements with chamber measurements and the Gas-Rover survey, the largest average methane fluxes appear to coincide with the areas of emission identified to the north and northwest of the tower, as well as to the southeast. When the tower was moved to site 2, the greatest average methane flux came from the emission area to the southwest of the tower (Figure 3). The emission area northeast of the tower had a surprisingly small average flux, especially considering that the area was sufficiently sampled due to frequent winds from that direction. However, winds most frequently came from the northeast at night, and increased stability and a smaller flux footprint may have prevented frequent sampling of the hot spot located northeast of the tower.

While the magnitude of methane fluxes measured in the farm field depends upon the spatial scale at which we are measuring, flux measurements made at a site level via eddy covariance and at a small scale via flux chambers are generally consistent. Eddy covariance measurements show a mean flux of 1.3 μmol m^{-2} s^{-1} with a range from −2.2 to 8.5 μmol m^{-2} s^{-1}. Chamber flux measurements range from 0 to 21 μmol m^{-2} s^{-1} with a mean flux of 1.7 μmol m^{-2} s^{-1}. The difference in the range of fluxes measured by each method is likely due to the spatial scales of the different measurements; in particular, the eddy covariance method smooths out the very high emissions from small areas. Chamber flux measurements also generally supported the spatial pattern of emissions shown in the eddy covariance data (Figure S14).

Proxy Flux Map. The multiplicative factor used to convert measurements of the methane mole fraction enhancement to a proxy flux, α, had a similar mean value when calculated using flux data from each of the two different flux tower locations. This supports our assumption that methane mole fraction enhancements and methane emissions are correlated (eq 3). α at site 1 (site 2) was 0.63 (0.52) μmol ppm^{-1} m^{-2} s^{-1} when calculated on a 0.5 m × 0.5 m grid. When calculated on a 1 m × 1 m grid, the average value of α at site 1 (site 2) was 0.64 (0.51) μmol ppm^{-1} m^{-2} s^{-1}, differing from the calculations on a 0.5 m × 0.5 m grid by only 0.01 μmol ppm^{-1} m^{-2} s^{-1}. The magnitudes of the proxy flux maps from site 1 and site 2 only differ slightly since the conversion factors calculated for the two different tower deployments only differ slightly (Figure S20). Fluxes measured using chambers fall within the distribution of calculated proxy fluxes (Figure S21). Proxy fluxes are shown at grid cells where the methane flux was measured using chambers in Table S2. While chamber flux data and the near-surface mole fraction map compare well qualitatively, there is some mismatch between the fluxes measured with chambers and proxy fluxes (Table S2). This mismatch is likely due to errors in upscaling point measurements to be representative of an area, errors within the GPS, or poor temporal sampling. We further tested the validity of our assumptions in calculations of α by examining its dependence on wind speed (Figure S18) and wind direction (Figure S19). We observe no dependence upon wind speed (Figure S18), although we do observe variation in α by wind direction. To account for this uncertainty in calculations of α, we estimate a range of potential site-wide emission rates using values from the 10th and 90th percentiles of the distribution of α calculated at each half-hour.

Temporal Pattern of Fluxes. *Eddy Covariance Fluxes.* Given sufficient sampling time in which many wind directions and stability conditions are sampled in a heterogeneous source area, temporal trends in methane fluxes may be discernible through eddy covariance measurements (e.g., Figure 4 and Table S1). Methane fluxes measured via eddy covariance did not appear to have any readily discernible temporal pattern (Figures 4 and S9), and monthly mean emissions were similar between all months (Table S1). We found no correlation between fluxes and precipitation or fluxes and water level as

https://doi.org/10.1021/acsearthspacechem.1c00312
ACS Earth Space Chem. 2022, 6, 909−919

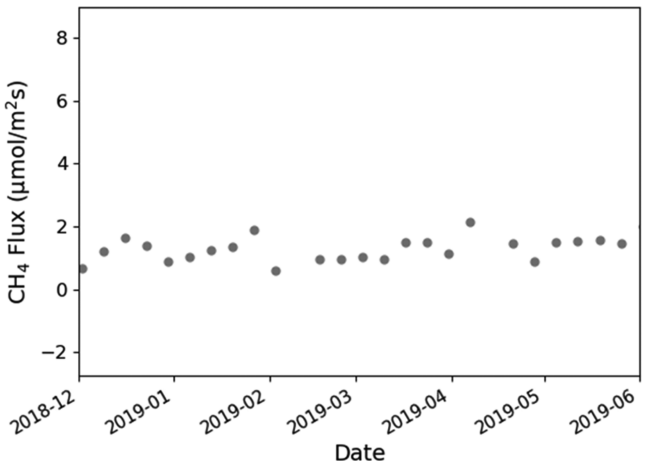

Figure 4. Weekly mean methane fluxes (μmol m^{-2} s^{-1}) from December 1st, 2018 to May 31st, 2019. The eddy covariance flux tower was moved from site 1 to site 2 on April 2nd, 2019.

measured by the closest USGS stream gage. We also did not see a clear temporal trend in α at the monthly scale (Figure S16) or a persistent pattern in the daily cycle of α (Figure S17), supporting our finding that there are no readily discernible temporal patterns in fluxes since α accounts for variations in wind direction and stability by incorporating the flux footprint.

Upscaling and Areally Integrated Site Flux. Best estimates of the integrated emissions from the 30 m radius circular study area fall within the range of 5−7 kg day^{-1} (Table 2). The methane emission from the 2,800 m^2 domain centered at tower site 1 is 6.57 kg day^{-1} (Table 2). Using the 10th and 90th percentiles of the distribution of values of α (Figure S15) produces a range of uncertainty of 1.66−13.97 kg day^{-1}. The site level methane emission from the 30 m radius circle centered at tower site 2 is 5.62 kg day^{-1}, with a similarly calculated range of uncertainty of 2.03−10.47 kg day^{-1}. When calculating site level methane emissions using individual mole fraction enhancement maps instead of the averaged map and the mean α value for each mole fraction enhancement map, emissions range from 5.8 to 8.7 kg/day (Table 2).

Table 2. Site Level Methane Emissions Calculated by Integrating Proxy Flux Maps[a]

site	mole fraction map	overall flux (kg day^{-1})	average α (μmol ppm^{-1} m^{-2} s^{-1})
1	average	6.57 [1.66−13.97]	0.63
2	average	5.62 [2.03−10.47]	0.52
1	1	8.70	0.87
2	1	8.04	0.72
1	2	8.55	1.37
2	2	5.77	0.83
1	3	7.11	0.71
2	3	6.11	0.64

[a]Proxy flux maps were centered at one of the two flux tower sites and created with one of the three methane mole fraction enhancement maps or an averaged map. Each methane mole fraction map is interpolated onto a 0.5 m × 0.5 m resolution grid. An estimate of uncertainty for each integrated flux estimate is provided by calculating an overall emission using values of α (μmol ppm^{-1} m^{-2} s^{-1}) that fall within 10 and 90% of the distribution.

These emission estimates only represent a portion of the total emissions from this event. Methane emissions can be found at other locations across this landscape, both within other parts of the field we measure and at other locations nearby.[27] We observed various other patches of dead vegetation within the field outside of our area of study. In the domain of our surveys of the enhancement of the methane mole fraction, we found that areas of dead vegetation were often colocated with areas of enhanced surface-level methane mole fraction (Figure 1). This suggests that other areas of dead vegetation within the field are additional locations of methane emissions. We also did not study emissions from the nearby stream, Gregs Run. The observed bubbling from the stream strongly suggests that methane could be upwelling into the water or along with the water. Thus, while we compare the magnitude of emissions we found from our small area of study with other sources, we do not have a comprehensive estimate of total emissions from this region and the impact of this potential stray gas migration may be much larger than our estimates. These results represent a first attempt to quantify surface methane emissions likely from stray gas migration. We compare the magnitude of the emissions we have measured with emissions estimated from nearby measurements of stream methane concentration as well as other methane sources associated with natural gas extraction in Pennsylvania for context.

Methane emission rates estimated from nearby stream surfaces are similar to or less than the range of emissions observed at the farm field near Gregs Run. Grieve et al. measured the methane concentration in the nearby stream named "Sugar Run" and estimated the influx of methane into the stream from the subsurface.[21,26] Those studies use a mass balance argument to estimate that a methane flux of 290−740 mg m^{-2} day^{-1} (0.2−0.5 μmol m^{-2} s^{-1}) enters Sugar Run along the study reach of the stream, totaling between 0.7 and 1.8 kg day^{-1}. That estimate uses the surface area of the stream channel as the collection area for the gas in the stream, which ultimately emits into the atmosphere.[21] However, if converging and upwelling groundwater carried methane from the entire area of the catchment into the stream, a more conservative estimate of the landscape area-normalized flux would use the area of the drainage area upstream of the sample instead of the area of the stream (0.127 mg m^{-2} day^{-1} or 9 × 10^{-5} μmol m^{-2} s^{-1}).

We now seek to place these fluxes in context. Leakage from natural gas systems can occur at many points during the extraction and transportation process, any of which can emit methane into the atmosphere.[15] For example, Omara et al. report that the average shale gas well in PA emits around 451.2 kg CH$_4$ day^{-1} (0.13% of production).[51] A different study by Caulton et al. found that the average unconventional well pad in Pennsylvania emits 132 kg day^{-1}.[16] The aforementioned study by Omara et al. showed that the average conventional gas well (a vertical well not completed using high-pressure high-volume hydraulic fracturing) emits 19.68 kg CH$_4$ h^{-1} (11% of production).[51] On the other hand, a high percentage of emissions from natural gas extraction can come from a small number of high-emitting unconventional wells that emit up to 360 kg h^{-1} or 8,640 kg day^{-1}: in other words, the distribution of emissions from sampling many wells is positively skewed.[16,17] In addition, in long-developed hydrocarbon-rich basins such as Pennsylvania, there are not only very large numbers of older conventional oil and gas wells but also a high

https://doi.org/10.1021/acsearthspacechem.1c00312
ACS Earth Space Chem. 2022, 6, 909−919

density of orphaned/abandoned oil and gas wells.[52] In a 2014 study, Kang et al. estimated that emissions from abandoned oil and gas wells may comprise as much as 4−6% of anthropogenic methane emissions in Pennsylvania.[53] Kang et al. measured emissions from 88 abandoned oil and gas wells, and they report a mean methane flow rate of 0.53 kg day^{-1} for an unplugged well and 0.36 kg day^{-1} for a plugged well.[52] At the unplugged gas well with the highest emissions, Kang et al. report an average emission rate of 1.8 kg day^{-1}.[52]

Although reports have documented stray gas migration events in Pennsylvania like the one we have studied,[54] no investigations have quantified the number of such stray gas migration events that result in atmospheric methane emissions kilometers from the well pad. Some studies suggest that stray gas migration into groundwater is fairly rare; one study highlighting Bradford county to the northeast suggests that 5 of 1,385 unconventional wells may have caused methane to leak into shallow aquifers.[55] We are unable to estimate the total emissions from the putatively leaking well discussed in this study. More extensive spatial and temporal sampling throughout the entire farm field, as well as knowledge of the spatial structure of emission sources, would be needed to constrain the magnitude of emissions from this event. This would also aid in further consideration of the significance of this source in the context of other methane emission sources. Documentation of the frequency of events like this one would also be needed to estimate the overall impact on methane emissions in the state. There may be as many as 750,000 abandoned oil and gas wells in Pennsylvania,[52] while there are over 12,000 active unconventional wells.[56] Between 2008−2021, 499 wells have received citations from the Pennsylvania Department of Environmental Protection targeting well casing issues. However, without knowledge of the frequency of stray gas migration events and the number of ongoing problematic wells, it is difficult to compare our emission estimate to these other sources.

In this work, we show that stray gas emission from shale gas wells can not only contaminate groundwater but can also emit methane directly into the atmosphere. Our method can be used to quantify similarly heterogeneous field-scale emissions. We show that the emissions from our case study of suspected stray gas migration are significant compared to other sources associated with natural gas extraction in PA, such as abandoned wells, but much smaller than the largest emissions from active production facilities. Emissions from the site we study appear to be consistent over several months of data collection. Emissions exhibit a highly heterogeneous spatial structure, perhaps associated with gas migration through subsurface features. Quantification of total emissions from this event would benefit from a more quantitative understanding of the subsurface migration pathways that the gas might follow. It is clear that we have only quantified a fraction of total emissions from this event. This work highlights an example of atmospheric methane emissions from potential stray gas migration at a location far from a well pad, and further research should explore the frequency and mechanisms behind these types of events to inform careful and strategic natural gas development.

■ ASSOCIATED CONTENT

Supporting Information

The Supporting Information is available free of charge at https://pubs.acs.org/doi/10.1021/acsearthspacechem.1c00312.

Measurements of the $\delta^{13}CH_4$ isotopic ratio and a Keeling plot; additional figures detailing methane emission location surveys and the gridded and averaged map; additional details about eddy covariance flux calculations and wind climatology at the site; analysis of potential impacts of drainage flow on fluxes; a flux footprint climatology; additional eddy covariance flux figures with all measurements for the entire time period and separated by month and hour; chamber construction details and testing; a map of chamber fluxes; additional analysis of the conversion factor α; proxy flux maps; and comparison of proxy flux maps with chamber fluxes (PDF)

■ AUTHOR INFORMATION

Corresponding Author

Kenneth J. Davis − *Department of Meteorology and Atmospheric Science, The Pennsylvania State University, University Park, Pennsylvania 16802, United States; Earth and Environmental Systems Institute, The Pennsylvania State University, University Park, Pennsylvania 16802, United States*; Email: kjd10@psu.edu

Authors

Lauren E. Dennis − *Department of Meteorology and Atmospheric Science, The Pennsylvania State University, University Park, Pennsylvania 16802, United States;* orcid.org/0000-0003-4384-4222

Scott J. Richardson − *Department of Meteorology and Atmospheric Science, The Pennsylvania State University, University Park, Pennsylvania 16802, United States*

Natasha Miles − *Department of Meteorology and Atmospheric Science, The Pennsylvania State University, University Park, Pennsylvania 16802, United States*

Josh Woda − *Department of Geosciences, The Pennsylvania State University, University Park, Pennsylvania 16802, United States*

Susan L. Brantley − *Department of Geosciences, The Pennsylvania State University, University Park, Pennsylvania 16802, United States; Earth and Environmental Systems Institute, The Pennsylvania State University, University Park, Pennsylvania 16802, United States;* orcid.org/0000-0002-9574-2693

Complete contact information is available at: https://pubs.acs.org/10.1021/acsearthspacechem.1c00312

Author Contributions

The manuscript was primarily written by L.E.D. and edited by all authors. All authors have given approval to the final version of the manuscript. L.E.D., S.J.R., N.M., and J.W. carried out the fieldwork and measurements. K.J.D. and S.L.B. supervised the work and conceived of the initial idea for the project. Measurement techniques were conceived by L.E.D., S.J.R., N.M., and K.J.D.

Funding

This work was funded by the National Science Foundation IIS Award # 1639150 to S.L.B. and Z. Li (Pennsylvania State

University), by Penn State's Institutes for Energy and the Environment, and by the Penn State College of Earth and Mineral Science's Earth and Environmental Systems Institute.

Notes

The authors declare no competing financial interest.

Data sets and analysis supporting this work can be found at: https://doi.org/10.26208/vsrv-0a97.

■ ACKNOWLEDGMENTS

The authors acknowledge the many homeowners who provided access to private land in the Sugar Run and Gregs Run valleys. The authors would like to thank Robert Ziegler for his assistance with instrument deployment and many Penn State students for assisting with fieldwork.

■ REFERENCES

(1) IPCC. *Climate Change 2014: Synthesis Report*; IPCC: Geneva, Switzerland, 2014.

(2) Masson-Delmotte, V.; Zhai, P.; Pörtner, H.-O.; Roberts, D.; Skea, J.; Shukla, P. R.; Pirani, A. *Global Warming of 1.5 °C. An IPCC Special Report on the Impacts of Global Warming of 1.5 °C above Pre-Industrial Levels and Related Global Greenhouse Gas Emission Pathways, in the Context of Strengthening the Global Response to the Threat of Climate Change*; Ipcc - Sr15, 2018; pp 17−20.

(3) Dlugokencky, E. J. Global CH_4 Monthly Means. *NOAA/ESRL*, 2018. https://gml.noaa.gov/ccgg/trends_ch4/.

(4) Saunois, M.; Bousquet, P.; Poulter, B.; Peregon, A.; Ciais, P.; Canadell, J. G.; Dlugokencky, E. J.; Etiope, G.; Bastviken, D.; Houweling, S.; et al. The Global Methane Budget 2000-2012. *Earth Syst. Sci. Data* **2016**, *8*, 697−751.

(5) Saunois, M.; Stavert, A. R.; Poulter, B.; Bousquet, P.; Canadell, J. G.; Jackson, R. B.; Raymond, P. A.; Dlugokencky, E. J.; Houweling, S.; Patra, P. K.; et al. The Global Methane Budget 2000−2017. *Earth Syst. Sci. Data* **2020**, *12*, 1561−1623.

(6) Wang, Q.; Chen, X.; Jha, A. N.; Rogers, H. Natural Gas from Shale Formation − The Evolution, Evidences and Challenges of Shale Gas Revolution in United States. *Renewable Sustainable Energy Rev.* **2014**, *30*, 1−28.

(7) Alvarez, R. A.; Zavala-Araiza, D.; Lyon, D. R.; Allen, D. T.; Barkley, Z. R.; Brandt, A. R.; Davis, K. J.; Herndon, S. C.; Jacob, D. J.; Karion, A.; et al. Assessment of Methane Emissions from the U.S. Oil and Gas Supply Chain. *Science* **2018**, *361*, 186−188.

(8) Barkley, Z. R.; Davis, K. J.; Feng, S.; Cui, Y. Y.; Fried, A.; Weibring, P.; Richter, D.; Walega, J. G.; Miller, S. M.; Eckl, M.; et al. Analysis of Oil and Gas Ethane and Methane Emissions in the Southcentral and Eastern United States Using Four Seasons of Continuous Aircraft Ethane Measurements. *J. Geophys. Res.: Atmos.* **2021**, *126*, No. e2020JD034194.

(9) Etiope, G. Natural Gas Seepage. In *The Earth's Hydrocarbon Degassing*; Springer, 2015.

(10) Levi, M. Climate Consequences of Natural Gas as a Bridge Fuel. *Clim. Change* **2013**, *118*, 609−623.

(11) U.S. Energy Information Administration. *Annual Energy Outlook 2021*, 2021.

(12) Pennsylvania Department of Environmental Protection. *Oil and Gas Annual Report*, 2018.

(13) Carter, K. M.; Harper, J. A.; Schmid, K. W.; Kostelnik, J. Unconventional Natural Gas Resources in Pennsylvania: The Backstory of the Modern Marcellus Shale Play. *Environ. Geosci.* **2011**, *18*, 217−257.

(14) Barkley, Z. R.; Lauvaux, T.; Davis, K. J.; Deng, A.; Miles, N. L.; Richardson, S. J.; Cao, Y.; Sweeney, C.; Karion, A.; Smith, M.; et al. Quantifying Methane Emissions from Natural Gas Production in North-Eastern Pennsylvania. *Atmos. Chem. Phys.* **2017**, *17*, 13941−13966.

(15) Brandt, A. R.; Heath, G. A.; Kort, E. A.; O'Sullivan, F.; Pétron, G.; Jordaan, S. M.; Tans, P.; Wilcox, J.; Gopstein, A. M.; Arent, D.; et al. Methane Leaks from North American Natural Gas Systems. *Science* **2014**, *343*, 733−735.

(16) Caulton, D. R.; Lu, J. M.; Lane, H. M.; Buchholz, B.; Fitts, J. P.; Golston, L. M.; Guo, X.; Li, Q.; McSpiritt, J.; Pan, D.; et al. Importance of Superemitter Natural Gas Well Pads in the Marcellus Shale. *Environ. Sci. Technol.* **2019**, *53*, 4747−4754.

(17) Omara, M.; Zimmerman, N.; Sullivan, M. R.; Li, X.; Ellis, A.; Cesa, R.; Subramanian, R.; Presto, A. A.; Robinson, A. L. Methane Emissions from Natural Gas Production Sites in the United States: Data Synthesis and National Estimate. *Environ. Sci. Technol.* **2018**, *52*, 12915−12925.

(18) Vidic, R. D.; Brantley, S. L.; Vandenbossche, J. M.; Yoxtheimer, D.; Abad, J. D. Impact of Shale Gas Development on Regional Water Quality. *Science* **2013**, *340*, No. 1235009.

(19) Pennsylvania Department of Environmental Protection. GHG Inventory https://www.dep.pa.gov/Citizens/climate/Pages/GHG-Inventory.aspx (accessed Jan 30, 2022).

(20) Pennsylvania Department of Environmental Protection. Oil and Gas Compliance - Report Extracts https://www.depgreenport.state.pa.us/ReportExtracts/OG/OilComplianceReport (accessed Jan 17, 2022).

(21) Grieve, P. L.; Hynek, S. A.; Heilweil, V.; Sowers, T.; Llewellyn, G.; Yoxtheimer, D.; Solomon, D. K.; Brantley, S. L. Using Environmental Tracers and Modelling to Identify Natural and Gas Well-Induced Emissions of Methane into Streams. *Appl. Geochem.* **2018**, *91*, 107−121.

(22) Brantley, S. L.; Yoxtheimer, D.; Arjmand, S.; Grieve, P.; Vidic, R.; Pollak, J.; Llewellyn, G. T.; Abad, J.; Simon, C. Water Resource Impacts during Unconventional Shale Gas Development: The Pennsylvania Experience. *Int. J. Coal Geol.* **2014**, *126*, 140−156.

(23) Osborn, S. G.; Vengosh, A.; Warner, N. R.; Jackson, R. B. Methane Contamination of Drinking Water Accompanying Gas-Well Drilling and Hydraulic Fracturing. *Proc. Natl. Acad. Sci. U.S.A.* 8172 8176. DOI: 10.1073/pnas.1100682108.

(24) Forde, O. N.; Mayer, K. U.; Cahill, A. G.; Mayer, B.; Cherry, J. A.; Parker, B. L. Vadose Zone Gas Migration and Surface Effluxes after a Controlled Natural Gas Release into an Unconfined Shallow Aquifer. *Vadose Zone J.* **2018**, *17*, No. 180033.

(25) Heilweil, V. M.; Grieve, P. L.; Hynek, S. A.; Brantley, S. L.; Solomon, D. K.; Risser, D. W. Stream Measurements Locate Thermogenic Methane Fluxes in Groundwater Discharge in an Area of Shale-Gas Development. *Environ. Sci. Technol.* **2015**, *49*, 4057−4065.

(26) Heilweil, V. M.; Risser, D. W.; Conger, R. W.; Grieve, P. L.; Hynek, S. A. *Estimation of Methane Concentrations and Loads in Groundwater Discharge to Sugar Run*, Open-File Report; Lycoming County, Pennsylvania, 2014.

(27) Woda, J.; Wen, T.; Oakley, D.; Yoxtheimer, D.; Engelder, T.; Castro, M. C.; Brantley, S. L. Detecting and Explaining Why Aquifers Occasionally Become Degraded near Hydraulically Fractured Shale Gas Wells. *Proc. Natl. Acad. Sci. U.S.A.* **2018**, *115*, No. 201809013.

(28) Grieve, P. L.; Hynek, S. A.; Heilweil, V.; Sowers, T.; Llewellyn, G.; Yoxtheimer, D.; Solomon, D. K.; Brantley, S. L. Using Environmental Tracers and Modelling to Identify Natural and Gas Well-Induced Emissions of Methane into Streams. *Appl. Geochem.* **2018**, *91*, 107−121.

(29) Wen, T.; Woda, J.; Marcon, V.; Niu, X.; Li, Z.; Brantley, S. L. Exploring How to Use Groundwater Chemistry to Identify Migration of Methane near Shale Gas Wells in the Appalachian Basin. *Environ. Sci. Technol.* **2019**, *53*, 9317−9327.

(30) The Pennsylvania Environmental Hearing Board. Case Number: 2015077, 2017.

(31) Powdermill GIS Lab. Powdermill Nature Reserve Maps and Geographic Information Systems https://maps.carnegiemnh.org/index.php/projects/unconventional-wells/download/ (accessed Aug 26, 2019).

(32) Pennsylvania Department of Environmental Protection. *Water Supply Determination Letters*, 2019.

(33) Schwietzke, S.; Sherwood, O. A.; Bruhwiler, L. M. P.; Miller, J. B.; Etiope, G.; Dlugokencky, E. J.; Michel, S. E.; Arling, V. A.; Vaughn, B. H.; White, J. W. C.; et al. Upward Revision of Global Fossil Fuel Methane Emissions Based on Isotope Database. *Nature* **2016**, *538*, 88−91.
(34) Baldassare, F. J.; McCaffrey, M. A.; Harper, J. A. A Geochemical Context for Stray Gas Investigations in the Northern Appalachian Basin: Implications of Analyses of Natural Gases from Neogene-through Devonian-Age Strata. *Am. Assoc. Pet. Geol. Bull.* **2014**, *98*, 341−372.
(35) Dlugokencky, E. J.; Nisbet, E. G.; Fisher, R.; Lowry, D. Global Atmospheric Methane: Budget, Changes and Dangers. *Philos. Trans. R. Soc., A* **2011**, *369*, 2058−2072.
(36) Rella, C. W.; Hoffnagle, J.; He, Y.; Tajima, S. Local- and Regional-Scale Measurements of CH4, Δ13CH4, and C2H6 in the Uintah Basin Using a Mobile Stable Isotope Analyzer. *Atmos. Meas. Tech.* **2015**, *8*, 4539−4559.
(37) Miles, N. L.; Martins, D. K.; Richardson, S. J.; Rella, C. W.; Arata, C.; Lauvaux, T.; Davis, K. J.; Barkley, Z. R.; McKain, K.; Sweeney, C. Calibration and Field Testing of Cavity Ring-down Laser Spectrometers Measuring CH_4, CO_2, and $\delta^{13}CH_4$ Deployed on Towers in the Marcellus Shale Region. *Atmos. Meas. Tech.* **2018**, *11*, 1273−1295.
(38) Rella, C. W.; Tsai, T. R.; Botkin, C. G.; Crosson, E. R.; Steele, D. Measuring Emissions from Oil and Natural Gas Well Pads Using the Mobile Flux Plane Technique. *Environ. Sci. Technol.* **2015**, *49*, 4742−4748.
(39) Keeling, C. D. The Concentration and Isotopic Abundances of Atmospheric Carbon Dioxide in Rural Areas. *Geochim. Cosmochim. Acta* **1958**, *13*, 322−334.
(40) Isotech Laboratories. *Collection of Ground Water Samples from Domestic and Municipal Water Wells for Dissolved Gas Analysis Using IsoFlasks*; 2011.
(41) Gas-Rover I and II | Bascom-Turner Instruments https://www.bascomturner.com/gas-rover-i-and-ii (accessed Nov 26, 2021).
(42) Fratini, G.; Mauder, M. Towards a Consistent Eddy-Covariance Processing: An Intercomparison of EddyPro and TK3. *Atmos. Meas. Tech.* **2014**, *7*, 2273−2281.
(43) LI-COR Biosciences. Eddy Covariance Processing Software. 2017.
(44) Kljun, N.; Rotach, M. W.; Schmid, H. P. A three-dimensional backward Lagrangian footprint model for a wide range of boundary-layer stratifications. In *Boundary-Layer Meteorology*; Springer, 2002; Vol. *103*, pp 205−226.
(45) Kljun, N.; Calanca, P.; Rotach, M. W.; Schmid, H. P. A Simple Two-Dimensional Parameterisation for Flux Footprint Prediction (FFP). *Geosci. Model Dev.* **2015**, *8*, 3695−3713.
(46) National Centers for Environmental Prediction/National Weather Service/NOAA/U.S. Department of Commerce. NCEP North American Regional Reanalysis (NARR). Research Data Archive at the National Center for Atmospheric Research, Computational and Information Systems Laboratory: Boulder, CO 2005.
(47) Parkin, T. B.; Venterea, R. T. USDA-ARS GRACEnet Project Protocols Chapter 3. Chamber-Based Trace Gas Flux Measurements 4 November 2010 (Replaces Original Version of April 2003). *Sampling Protocols* **2010**, *2010*, 3.1−3.39.
(48) Kim, J.; Guo, Q.; Baldocchi, D. D.; Leclerc, M. Y.; Xu, L.; Schmid, H. P. Upscaling Fluxes from Tower to Landscape: Overlaying Flux Footprints on High-Resolution (IKONOS) Images of Vegetation Cover. *Agric. For. Meteorol.* **2006**, *136*, 132−146.
(49) Sutherland, G.; Chasmer, L. E.; Petrone, R. M.; Kljun, N.; Devito, K. J. Evaluating the Use of Spatially Varying versus Bulk Average 3D Vegetation Structural Inputs to Modelled Evapotranspiration within Heterogeneous Land Cover Types. *Ecohydrology* **2014**, *7*, 1545−1559.
(50) Werner, C.; Brantley, S. CO2 emissions from the Yellowstone Volcanic System. In *Geochemistry, Geophysics, Geosystems*; Wiley, 2003; Vol. *4*.
(51) Omara, M.; Sullivan, M. R.; Li, X.; Subramian, R.; Robinson, A. L.; Presto, A. A. Methane Emissions from Conventional and Unconventional Natural Gas Production Sites in the Marcellus Shale Basin. *Environ. Sci. Technol.* **2016**, *50*, 2099−2107.
(52) Kang, M.; Christian, S.; Celia, M. A.; Mauzerall, D. L.; Bill, M.; Miller, A. R.; Chen, Y.; Conrad, M. E.; Darrah, T. H.; Jackson, R. B. Identification and Characterization of High Methane-Emitting Abandoned Oil and Gas Wells. *Proc. Natl. Acad. Sci. U.S.A.* **2016**, *113*, 13636−13641.
(53) Kang, M.; Kanno, C. M.; Reid, M. C.; Zhang, X.; Mauzerall, D. L.; Celia, M. A.; Chen, Y.; Onstott, T. C. Direct Measurements of Methane Emissions from Abandoned Oil and Gas Wells in Pennsylvania. *Proc. Natl. Acad. Sci. U.S.A.* **2014**, *111*, 18173−18177.
(54) Llewellyn, G. T.; Dorman, F.; Westland, J. L.; Yoxtheimer, D.; Grieve, P.; Sowers, T.; Humston-Fulmer, E.; Brantley, S. L. Evaluating a Groundwater Supply Contamination Incident Attributed to Marcellus Shale Gas Development. *Proc. Natl. Acad. Sci.. U.S.A.* **2015**, *112*, 6325−6330.
(55) Wen, T.; Niu, X.; Gonzales, M.; Zheng, G.; Li, Z.; Brantley, S. L. Big Groundwater Data Sets Reveal Possible Rare Contamination Amid Otherwise Improved Water Quality for Some Analytes in a Region of Marcellus Shale Development. *Environ. Sci. Technol.* **2018**, *52*, 7149−7159.
(56) DEP Office of Oil and Gas Management. *Operator Well Inventory Report*, 2020.

https://doi.org/10.1021/acsearthspacechem.1c00312
ACS Earth Space Chem. 2022, 6, 909−919